IEEE Access
Multidisciplinary | Rapid Review | Open Access Journal

Received July 3, 2020, accepted July 20, 2020, date of publication July 27, 2020, date of current version August 11, 2020.

Digital Object Identifier 10.1109/ACCESS.2020.3012119

An Efficient Control Strategy for Enhancing Frequency Stability of Multi-Area Power System Considering High Wind Energy Penetration

MOHAMED KHAMIES[1], GABER MAGDY[2], MOHAMED EBEED HUSSEIN[3], FAHD A. BANAKHR[4], (Member, IEEE), AND SALAH KAMEL[1]

[1]Department of Electrical Engineering, Faculty of Engineering, Aswan University, Aswan 81542, Egypt
[2]Department of Electrical Engineering, Faculty of Energy Engineering, Aswan University, Aswan 81528, Egypt
[3]Department of Electrical Engineering, Faculty of Engineering, Sohag University, Sohag 82524, Egypt
[4]Department of Electrical and Electronic Engineering, Yanbu Industrial College, Yanbu 46452, Saudi Arabia

Corresponding authors: Fahd A. Banakhr (banakhrf@rcyci.edu.sa) and Salah Kamel (skamel@aswu.edu.eg)

This work was supported by the Chilean Council of Scientic and Technological Research under Grant ANID/Fondap/15110019.

ABSTRACT This paper proposes an efficient control strategy to enhance frequency stability of three-area power system considering a high penetration level of wind energy. The proposed strategy is based on a combination of a Proportional Integral Derivative (PID) controller with a Linear Quadratic Gaussian (LQG) approach. The parameters of the proposed controller (i.e., PID-LQG) are optimally designed by a novel natural physical based-algorithm called Lightning Attachment Procedure Optimization (LAPO). The main objective is to keep the frequency fluctuation at its acceptable value in the presence of high penetration of wind energy, high load disturbance and system uncertainties. The superiority of the proposed PID-LQG controller is validated by comparing its performance with optimal Coefficient Diagram Method (CDM) controller, conventional CDM controller, optimal PID controller-based LAPO, and integral controller. Moreover, the exhaustive results completely demonstrate that the proposed controller gives better performance in terms of overshoot, undershoot, and settling time as well as provides reliable frequency stability for interconnected power systems considering high wind penetration and system uncertainties.

INDEX TERMS Frequency stability, interconnected power systems, linear quadratic Gaussian (LQG), lightning attachment procedure optimization (LAPO), high penetration of wind energy.

I. INTRODUCTION

The energy demand is gradually increasing which requires establishing renewable energy sources (RESs), transmission lines as well as interconnection among power system areas to meet future demands. Carbon reduction requires a large establishing of renewable generating units instead of generating units produce fossil fuels. Moreover, RESs are abundant, friendly to the environment, cheap, and clean [1]. Wind energy is considered one of the most consequential RESs, where its installation cost is less than the photovoltaic (PV) plants. Therefore, wind energy represents a larger segment of installed resources from renewable power plants [2]. In the context of planning to expand generation, the total price of electricity decreases when renewables power penetration increases in the power system [3], [4].

The associate editor coordinating the review of this manuscript and approving it for publication was Md Apel Mahmud.

With increasing the penetration level of RESs into the power systems, the impact of low system inertia on dynamic system performance and stability increases. In addition, the random nature of the RESs causes many control issues (e.g., frequency instability), that may restrict their high penetration [5]. Therefore, many efforts have been done to minimize the effect of the high penetration of RESs in the power system by determining the amount of required power from RESs. A Monte Carlo method based on the particle swarm optimization (PSO) algorithm is proposed to determine the power required of RESs to meet the load demand [6]. Also, a heuristic-based approach to load demand prediction is applied to determine the power needed from distributed energy sources (i.e. wind turbine generator, Photovoltaic (PV) system, energy storage systems) [7]. On the other hand, frequency fluctuations may result from unbalancing between the required power for the load and the supplied power from generation plants. Therefore, this issue has significant

influences on the electrical systems include their operation, reliability, security, transmission lines overloading, and the protection devices triggering [8]. Thus, these effects must be eliminated by enhancing frequency stability. Four control loops (i.e. primary control, secondary control, tertiary control, and emergency control) are responsible to enhance frequency stability and overcome any fluctuations that occur in the power system [9].

Various control approaches have been developed to enhance frequency stability and control unscheduled tie-line power divergence against system variations such as adaptive fuzzy logic controller [10], model predictive control (MPC) [11], adaptive neural network controller [12], an adaptive neuro-fuzzy controller [13], sliding mode control [14]. Though the above-mentioned controllers can successfully handle the system frequency deviation, they suffer from many shortcomings such as (i) its reliant on the designer experience to arrive at the right concept, (ii) its processing time is long, (iii) its complex procedures, and (iv) its high cost compared to traditional controllers. Admittedly, PID controllers are commonly used in industrial applications due to its simplest in structure, its lower cost compared to other control techniques [15]. However, the PID controllers are more sensitive to systems uncertainties. So, it is essential to design optimal PID controller whose parameters selected based optimization techniques to withstand any variations recently. Therefore, some optimization algorithms are employed to obtain the optimum PID controller gains such as; artificial bee colony algorithm (ABC) [16], salp swarm algorithm(SSA) [17], Improved sine cosine algorithm (ISCA) [18], Bacteria foraging optimization (BFO) [19], cuckoo search technique [20], bat inspired algorithm (BIA) [21], Moth-flame optimization (MFO) [22], bat algorithm (BA) [23], Jaya algorithm [24], and Elephant Herding Optimization (EHO) [25]. Although, these algorithms can able to obtain optimal parameters that lead to successful results, the shortage of these techniques is that they long elapsed time and very sensitive to their parameters.

On the other hand, various advanced robust control techniques have been applied for frequency stability of power systems. Where, robust control techniques have advantages in considering disturbances, uncertainties and physical constraints. According to this consideration, numerous studies related to application of the robust control for power system have been depicted [26]–[29]. In [26], a coefficient diagram (CDM) method is applied to a virtual inertia control loop to improve the frequency stability of an islanded microgrid considering a high penetration level of renewables. A robust control technique based on the H-infinity approach is applied for controlling frequency in an islanded microgrid considering RESs penetration [27]. Also, a robust controller-based μ synthesis for improving the stability of the microgrid considering energy storage system (ESS) [28]. In addition, the H-infinity approach is applied in combination with μ synthesis for the LFC problem in an islanded microgrid [29]. Based on the aforementioned robust controllers, the robust controllers have a drawback that they need to have a good knowledge of the system. In addition, they have weak effects with an unknown variable input.

A few researchers have prompted studies on optimal control techniques that their design based on minimizing of the cost function e.g. the linear quadratic regulator (LQR) for achieving the superior goal by keep frequency at acceptable range in power system have been presented in [30]–[35]. In [30] the LQR controller is applied in addition to Kalman filter (KF) to form (LQR-KF) to eliminate frequency fluctuations in an interconnected power system. Therefore, the LQR is applied in addition to Model predictive control (MPC) for eliminating the frequency deviation in small power system area considering generation rate constraint (GRC) and governor dead band (GDB) [31]. Moreover, the linear quadratic Gaussian (LQG) linked with MPC to improve frequency stability in power system depends on conventional generating unit [32]. The LQR is applied to a two-area interconnected area in smart grid design for regulating the frequency [33]. Moreover, a Kalman filter is proposed to form linear quadratic gaussian to diminish any deviation in frequency according to system uncertainties [34]. In [35] an effective integral linear quadratic gaussian (ILQG) controller is proposed to reduce the fluctuations in frequency response in two power system areas populated with Plug-in hybrid electric vehicles (PHEV).Although these approaches success to solve LFC problems, they depended on the designer experience and the trial and error methods to select the controller parameters.

Referring to the presented studies of the LFC topic, conventional controllers such that the PID controller suffer from difficulties in parameter selection. Moreover, few works focused on LQR and LQG controllers to solve the LFC issue. However, these few studies didn't consider any optimization algorithms for finding the LQR and LQG control parameters where they mostly used trial and error methods. On the other hand, there are few studies devoted to LFC considering high the RESs penetration in the interconnected power systems. Motived by the above observations, this study proposes a combination of the PID controller with the LQG approach, to obtain a robust PID-LQG controller for the frequency stability of a multi-area interconnected power system considering a high penetration level of wind energy and uncertainties. Moreover, the lightning Attachment Procedure Optimization (LAPO) algorithm is proposed to find the optimal parameters of the proposed PID-LQG controller. The LAPO algorithm presented by Nematollahi *et al.* [36]. This algorithm simulates the Lightning phenomena in nature. The LAPO is based on for steps which are: leader upward direction, section fading, downward leader orientation, and the strike point which mimics the optimal solution [37]. Therefore, it has high searching capability applied for solving several optimization problems. In [36], the LAPO algorithm is applied to determine the optimal power flow for power system. It is applied for the same issue in the presence of a unified power flow controller in [38]. Also, the LAPO algorithm is applied

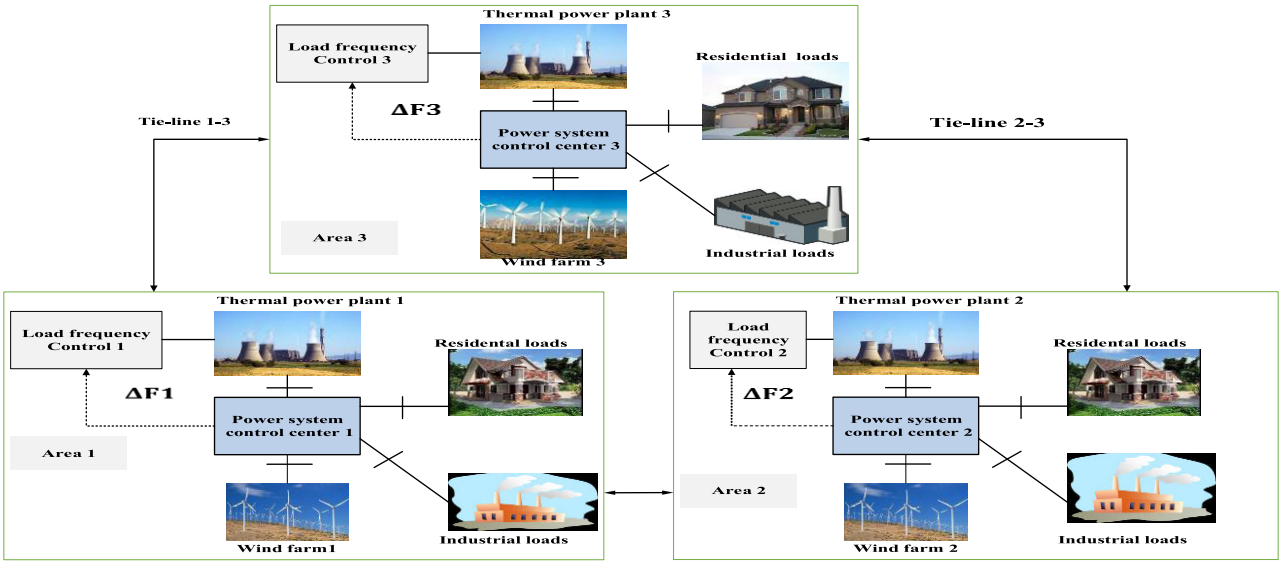

FIGURE 1. A simplified model of the studied three area interconnected power system.

to capture the optimal placement and size of the distributed generators in [39].

According to the above investigation, the main paper contributions and features are listed as follows:

i. Proposing a new control strategy based on a PID-LQG controller to diminish the deviation in frequency of the multi-area power system considering high penetration of wind energy.
ii. The proposed PID-LQG controller is based on the PID controller combine with the LQG controller to enhance frequency stability and face the high penetration of wind farms.
iii. The PID-LQG controller parameters are optimally assigned by implementation a new algorithm: called the LAPO algorithm, which hasn't applied yet to select the optimum parameters for the PID controller.
iv. It is the first attempt applying an optimization technique to select the parameters of the LQG controller, unlike the previous efforts, the design of the LQG controller parameters depends on the design experience with the use of trial and error method.
v. The system uncertainties such as the governor dead band (GDB), the generation rate constraint (GRC), and load/RESs fluctuations are considered in designing the proposed controller.
vi. This study considers the high-penetration level of wind power in the interconnected power system including the three-area power system, unlike most previous research have considered the penetration of RESs in the single-area power system.

The rest paper sections are arranged as follows. Section 2 presents the dynamical model of the studied power system, wind generation modelling, and the state-space dynamic equations. The proposed controller technique for the studied power system based on the LAPO algorithm is depicted in Section 3. The exhaustive simulation results are presented in Section 4. The conclusion is listed in Section 5.

II. SYSTEM MODELLING AND CONFIGURATION

A. DYNAMIC MODEL OF A THREE-AREA POWER SYSTEM

A three-area power system model is considered as the studied power system. The studied power system consists of three areas tied by tie-lines. Moreover, each area consists of a thermal generating unit, wind generating unit, and loads. The simplified model of the studied power system is shown in Figure 1. The dynamic model of the studied three-area interconnected power system with the proposed PID-LQG controller scheme is shown in Figure 2, and the system parameters are given in Table 1 [8]. Frequency measurement is considered an important pointer to control frequency in each area besides its role in the interconnection between areas. During abnormal conditions, the tie lines are connected to exchange power among the interconnected areas and furnish inter-area support. The mismatches should be adjusted by the supplementary control. Area control error (ACE) results from a combination of the frequency error (ΔF) and tie-line power error (ΔP_{tie}). This combination is the input of load frequency controllers which affects the area performance. The main task of the LFC system in each area is to handle tie-line power deviations and enhance frequency stability. Hence, the LFC problem should consider the tie-line power signal.

The relationship between the incremental mismatch power($\Delta P_{mi} - \Delta P_{Li} - \Delta P_{WTi}$) and the Δf_i can be express as:

$$\dot{\Delta f_i} = \left(\frac{1}{2H_i}\right)\Delta P_{mi} - \left(\frac{1}{2H_i}\right)\Delta P_{Li} - \left(\frac{D_i}{2H_i}\right)\Delta f_i - \left(\frac{1}{2H_i}\right)\Delta P_{tie,i} - \left(\frac{1}{2Hi}\right).\Delta P_{WTi} \quad (1)$$

whereas, the dynamic of the governor can be interpreted as:

$$\Delta \dot{P}_{mi} = \left(\frac{1}{T_{ti}}\right)\Delta P_{gi} - \left(\frac{1}{T_{ti}}\right)\Delta P_{mi} \quad (2)$$

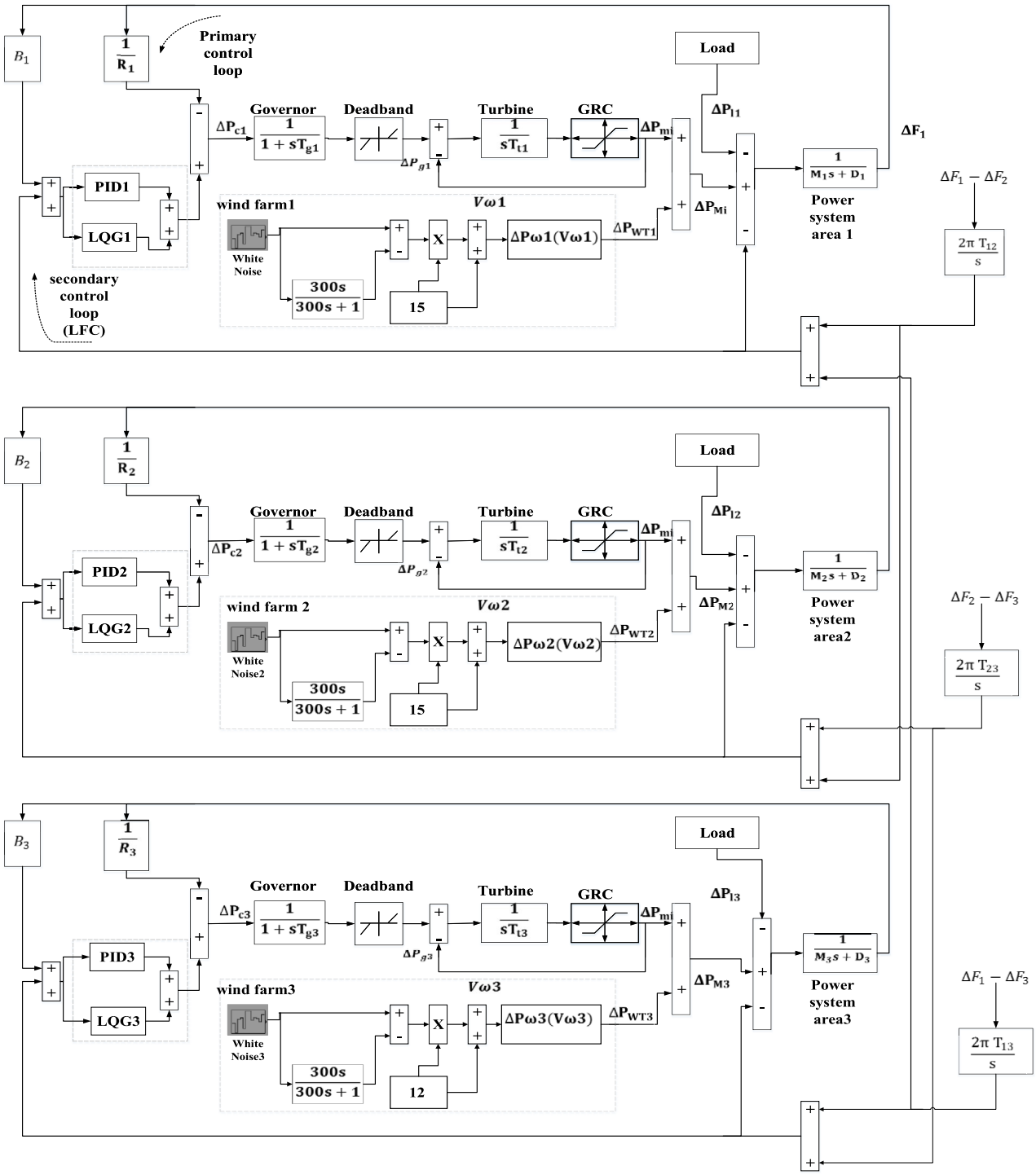

FIGURE 2. The dynamic model of the three-area interconnected power system.

The dynamic of the turbine can be interpreted as:

$$\Delta\dot{P}_{gi} = \left(\frac{1}{T_{gi}}\right)\Delta P_{ci} - \left(\frac{1}{R_i T_{gi}}\right)\Delta f_i - \left(\frac{1}{T_{gi}}\right)\Delta P_{gi} \quad (3)$$

Moreover, the dynamic model of wind turbine can be interpreted as:

$$\Delta\dot{P}_{WTi} = \left(\frac{1}{T_{WTi}}\right).P_{wind,i} - \left(\frac{1}{T_{WTi}}\right).\Delta P_{WT,i} \quad (4)$$

Then, the total tie-line power change can be expressed as follow:

$$\Delta\dot{P}_{tie,i} = 2\pi.\left[\sum_{\substack{j=1\\ j\neq i}}^{N} T_{ij}\Delta f_i - \sum_{\substack{j=1\\ j\neq i}}^{N} T_{ij}\Delta f_j\right] \quad (5)$$

In the supplementary feedback loop, ACE should be applied to regulate the frequency of interconnected power system.

TABLE 1. The studied power system nominal parameters.

Parameters	Area-1	Area-2	Area-3
D(pu MW /HZ)	0.015	0.016	0.015
2H(pu.MW s)	0.1667	0.2017	0.1247
R(Hz/pu.MW)	3.00	2.73	2.82
T_g (sec)	0.08	0.06	0.07
T_t (sec)	0.40	0.44	0.3
β(pu/HZ)	0.3483	0.3827	0.3692
T_{ij} (pu/HZ)	T12=0.2 T13=0.25	T21=0.2 T23=0.15	T31=0.25 T32=0.12

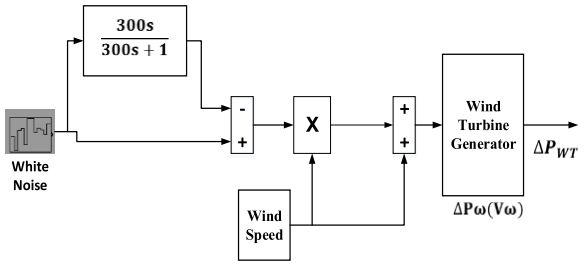

FIGURE 3. A model of wind power generating source.

ACE expressed as follow:

$$ACE_i = \Delta P_{tie,i} + B_i \Delta f_i \tag{6}$$

The state space model of power system area according (1) to (6), can calculated using (7), as shown at the bottom of the page.

The nonlinearity effect of this studied system is considered in two inherent nonlinearities. The GDB which has an effect on the governor unit and its value equals 0.05 pu for every area. While, the GRC is considered at a value of 10% for the turbine unit.

wherever, $v_i = \left[\sum_{\substack{j=1 \\ j \neq i}}^{N} T_{ij} \Delta f_j\right]$.

B. WIND FARM

The random wind power fluctuations result from wind farm accomplished by a model designed by MATLAB/ SIMULINK program. According to the designed model, random speed is multiplied by wind speed, which resulted by a white noise block as shown in Figure 3 [40]. Wind power generation system (WPGS) model is captured form the following equations [40]:

TABLE 2. The parameters of wind farms 1, and 2 [40].

Parameter	Value	Parameter	Value
P_w	750 KW	c_2	116
V_w	15m/s	c_3	0.4
ρ	1.225 kg.m3	c_4	0
A_T	1648m2	c_5	5
r_T	22.9 m	c_6	21
n_T	22.5 rpm	c_7	0.1405
c_1	-0.6175		

$$P_W = \frac{1}{2}\rho A_T V_W^3 C_P(\lambda, \beta) \tag{8}$$

wherever, P_W is wind turbine output power, ρ is air density in kg/m3, A_T is swept area by rotor in m2, V_W is rated wind speed in m/s. C_P denotes the rotor blades coefficient. Equation. (8) describes C_P based on turbine coefficients $C_1 - C_7$ [41].

$$C_P(\lambda, \beta) = C_1 \times \left(\frac{C_2}{\lambda_I} - C_3\beta - C_4\beta^2 - C_5\right) \times e^{\frac{-C_6}{\lambda_I}} + C_7\lambda_T \tag{9}$$

wherever, β denotes pitch angle while λ_T relates to the optimum tip-speed ratio (TSR) can be obtained from (9).

$$\lambda_T = \lambda_T^{OP} = \frac{\omega_T \times r_T}{V_W} \tag{10}$$

Throughout all wind speed situations, variable speed wind turbines run at optimum TSR value. Referring to previous equation, r_T represents rotor radius. Moreover, λ_I denotes the intermittent TSR which is given using (11).

$$\frac{1}{\lambda_I} = \frac{1}{\lambda_T + 0.08\beta} - \frac{0.035}{\beta^3 + 1} \tag{11}$$

The nominal parameters of wind turbine for three wind farms are given in Tables 2, and 3.

III. PROPOSED CONTROL STRATEGY AND PROBLEM FORMULATION

A. PROPOSED PID-LQG CONTROLLER

Due to the high-level penetration of wind energy and system uncertainties, it is important to propose a robust controller

$$\begin{bmatrix} \Delta\dot{P}_{gi} \\ \Delta\dot{P}_{mi} \\ \Delta\dot{F}_i \\ \Delta\dot{P}_{wT,i} \\ \Delta\dot{P}_{tie,i} \end{bmatrix} = \begin{bmatrix} \frac{-1}{T_{gi}} & 0 & \frac{-1}{Ri.T_{gi}} & 0 & 0 \\ \frac{1}{T_{ti}} & \frac{-1}{T_{ti}} & 0 & 0 & 0 \\ 0 & \frac{1}{2Hi} & \frac{-D}{2Hi} & \frac{-1}{2Hi} & \frac{-1}{2Hi} \\ 0 & 0 & 0 & \frac{-1}{T_{WTi}} & 0 \\ 0 & 0 & 2\pi \sum_{\substack{j=1 \\ j \neq i}}^{N} T_{ij} & 0 & 0 \end{bmatrix} \begin{bmatrix} \Delta P_{gi} \\ \Delta P_{mi} \\ \Delta F_i \\ \Delta P_{WTi} \\ \Delta P_{tiei} \end{bmatrix} + \begin{bmatrix} 0 & 0 & 0 \\ 0 & 0 & 0 \\ \frac{-1}{2Hi} & 0 & 0 \\ 0 & 0 & \frac{-1}{T_{WTi}} \\ 0 & 0 & -2\pi \end{bmatrix} \begin{bmatrix} \Delta P_{li} \\ \Delta v_i \\ \Delta P_{windi} \end{bmatrix} + \begin{bmatrix} \frac{1}{T_{gi}} \\ 0 \\ 0 \\ 0 \\ 0 \end{bmatrix} \Delta P_{ci} \tag{7}$$

TABLE 3. The parameters of wind farm 3 [40].

Parameter	Value	Parameter	Value
P_w	3000 KW	c_2	116
V_w	12 m/s	c_3	0.4
ρ	1.225 kg.m3	c_4	0
A_T	5905 m2	c_5	5
r_T	43.63 m	c_6	21
n_T	22.5 rpm	c_7	0.0192
c_1	0.3915		

to face these variations and improve system performance. Therefore, this study proposes a robust PID-LQG controller, which is a combination of the PID controller and the LQG controller to take the advantages of these two controllers. The PID controller is feasible and easy to be implemented. Where, the PID gains can be designed based upon the system parameters if they can be achieved precisely. However, the PID controller generally has to balance all three-gain impact on the whole system and may compromise the transient response, such as settling time, overshoots, and oscillations. If the system parameters cannot be precisely estimated, the designed PID gains may not resist the uncertainties and disturbances, and thus lead to low robustness. According to this limitation of the PID controller, the LQG controller is proposed to combine with the PID controller due to its major advantages as follow:

i. Providing a time-varying control signal in each moment which causes the system to follow the proper trajectory.
ii. Minimizing a cost function during transient periods while specifying a trade-off among the state regulation and control action.
iii. Robustness and possibility of choosing different controller configurations according to the non-uniqueness property of optimal control.

Therefore, the proposed controller can give high robustness compared to the PID controller alone due to the many aforementioned merits of the LQG controller. Moreover, the proposed controller has also advantaged of optimal control due to its ability in minimizing cost function and feedback control due to its ability to minimize feedback gain. The simplified block diagram of the proposed control strategy is shown in Figure 4. The proposed approach designing depends on the PID controller gains, LQR controller gains, and Kalman filter which is applied to measure all the state variables and avoiding the LQR limitations.

The proposed controller designing procedures is listed in the pseudocode in Table 4. Where the designing process depending on the following steps:

i. Design the PID controller.
ii. Design the LQR controller.
iii. Design a Kalman filter.
iv. Combining the LQR controller and Kalman filter gain to obtain the LQG controller.
v. Combine the PID controller and LQG controller to obtain the proposed controller (PID-LQG).

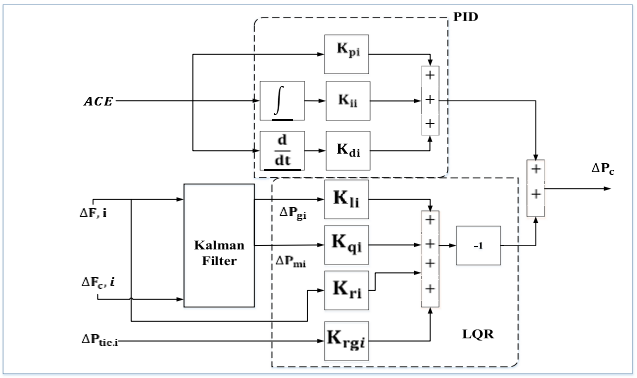

FIGURE 4. The block diagram of the proposed (PID-LQG) controller for i-area power system.

TABLE 4. PID-LQG pseudo code.

Construct the feedback gain and Kalman filter gain & check the stability of system
Identify the system data
Find the state space model of the system
Create the system matrix A, B and C according to system data.
Design the Kalman filter gain L.
Construct the weighting matrix Q.
Construct the controlling matrix R.
If Q≥0 and R>0
Capture the feedback gain K (k_l-k_q-k_r-k_{rg}).
Else,
Update the values for Q and R matrix.
Combine the two gains K and L to form optimal LQG.
Construct the PID controller gains k_p- k_i - k_d
Combine the PID controller gains and LQG controller gains
Check the system stability.
For all values of gains
If Stability of the system enhancement.
Keep the values of all gains
Else,
Update the values for Q and R matrix to update the LQR controller gains
Update the PID controller gains k_p- k_i - k_d
End if,
The gain values achieve stability of the system.
Identify the values of matrix Q and R and all designed gains

The PID controller is termed as follows according to [42]:

$$G_c(s) = k_p + \frac{k_i}{s} + k_d s. \tag{12}$$

Then, the LQG gains are selected by applying the state-space model of the system, and finding the value of optimal state feedback $u^*(t)$ through the following equation [43]:

$$u^*(t) = -K(t)\,x(t) \tag{13}$$

The state variable of the system is defined as follow:

$$\dot{x}(t) = Ax(t) + Bu(t) \tag{14}$$

Then, the output of the system is defined as follow:

$$Y(t) = Cx(t) + Du(t) \tag{15}$$

where A, B and C are the system matrixes and $u(t)$ is the control input. Moreover, the optimal gain matrix K of the

TABLE 5. The LAPO algorithm pseudo code.

Calculate the objective function for any check point
- *Define the parameters of algorithm (search agent numbers).*
- *Define the system data (lower, upper limit and objective function).*
- *Initialize the trial spots(x_{st}^i)*
- *Obtain the objective function of trial spots ($F_{obj}x_{st}^i$).*

Determine the mean point of check points and its objective function (F_{avr} and x_{avr}^i).

If
$F_{obj} < F_{avr}$.
Calculate the new value of trial spots as
$X_{ts_{new}}^i = X_{ts}^i + rand \times \left(X_{avr} + A_{PS}^j\right)$
Else,
Calculate the new value of trial spots as
$A_{ts\_new}^i = X_{ts}^i - rand \times \left(X_{avr} + X_{PS}^j\right)$

Diminishing the section to determine the new check points

If
$F_{ts\_new}^i < F_{ts}^i$
The new value is $X_{ts}^i = X_{ts\_new}^i$
Otherwise,
The new value is $X_{ts\_new}^i = X_{ts}^i$.

Determining the value of an exponent factor (S)
- *Find the objective function of the updated points.*
- *Determine the worst and best solutions* X_{worst}^i - X_{best}^i

Finding the optimal solution
Print the best solution

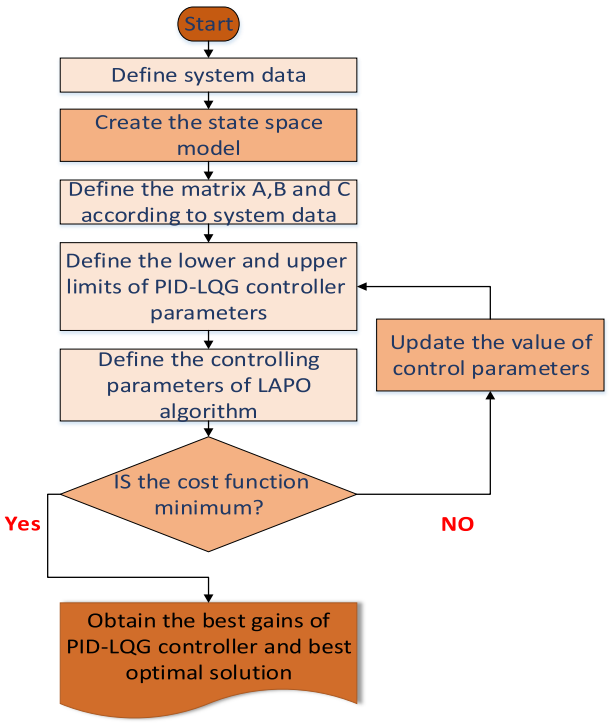

FIGURE 5. Flow chart of the proposed approach using LAPO algorithm.

LQR controller is calculated to diminish the cost function J as follows:

$$J = \int_{t^\circ}^{t_f} (\acute{x}Qx + u\acute{R}u + 2X\grave{N}u)dt \tag{16}$$

TABLE 6. LAPO algorithm initial values and limitations of the proposed controller gains.

Number of Test points	40
Number of iterations	100
Range of ($k_{pi} - k_{ii} - k_{di}$)	[5 -20]
Range of Q_i	[0 20]
Range of R_i	[0 150]

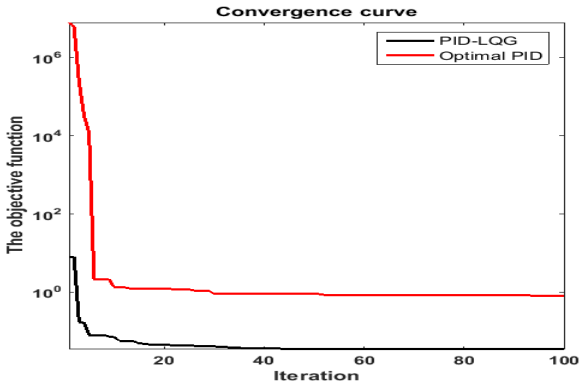

FIGURE 6. Convergence curve for normal system parameters.

Therefore, the constraint problem can be resolved by the n-vector of Lagrange multipliers, λ. The minimization of unconstrained problem is reduced as follows:

$$L(x, \lambda, u, t) = \left[\acute{x}Qx + \acute{u}Ru\right] + \acute{\lambda}[Ax + Bu - \dot{x}] \tag{17}$$

Moreover, the most fitted values symbolized by subscript (*). Then, they are obtained by equating the partial derivatives to zeros.

$$\frac{\partial L}{\partial \lambda} = Ax^* + Bu^* - \dot{x}^* = 0\dot{x}^* = Ax^* + Bu^* \tag{18}$$

$$\frac{\partial L}{\partial u} = 2Ru^* + \lambda\acute{B} = 0u^* = -\frac{1}{2}R^{-1}\lambda\acute{B} \tag{19}$$

$$\frac{\partial L}{\partial x} = 2\dot{x}^*Q + \dot{\lambda}\dot{+}\lambda\acute{A} = 0\lambda = -2\dot{Q}x^* - A\dot{\lambda} \tag{20}$$

Here, Q denotes the matrix of state weighting and R denotes the matrix control weighting. It is important to build the weighting matrix symmetric, real and positive semi definite. The matrix of control weighting real, symmetric and positive definite character. The time varying positive definite matrix $P(t)$ should satisfy:

$$\lambda = 2P(t)x^* \tag{21}$$

Then, the derivative of (21) as follows:

$$\dot{\lambda} = 2(P\dot{x}^* + P\dot{x}^*) \tag{22}$$

According to the values in, (13), the optimal closed-loop control law is given as depicted (23).

$$u^*(t) = -R^{-1}\acute{B}p(t)\,x^* \tag{23}$$

Solving the Riccati equation as follows:

$$\dot{P} = -P(t)A - \acute{A}P(t) - Q + P(t)BR^{-1}\acute{B}P(t)\,. \tag{24}$$

The optimal feed-back gain and the state response of the assumed system have been solved by solving the Riccati

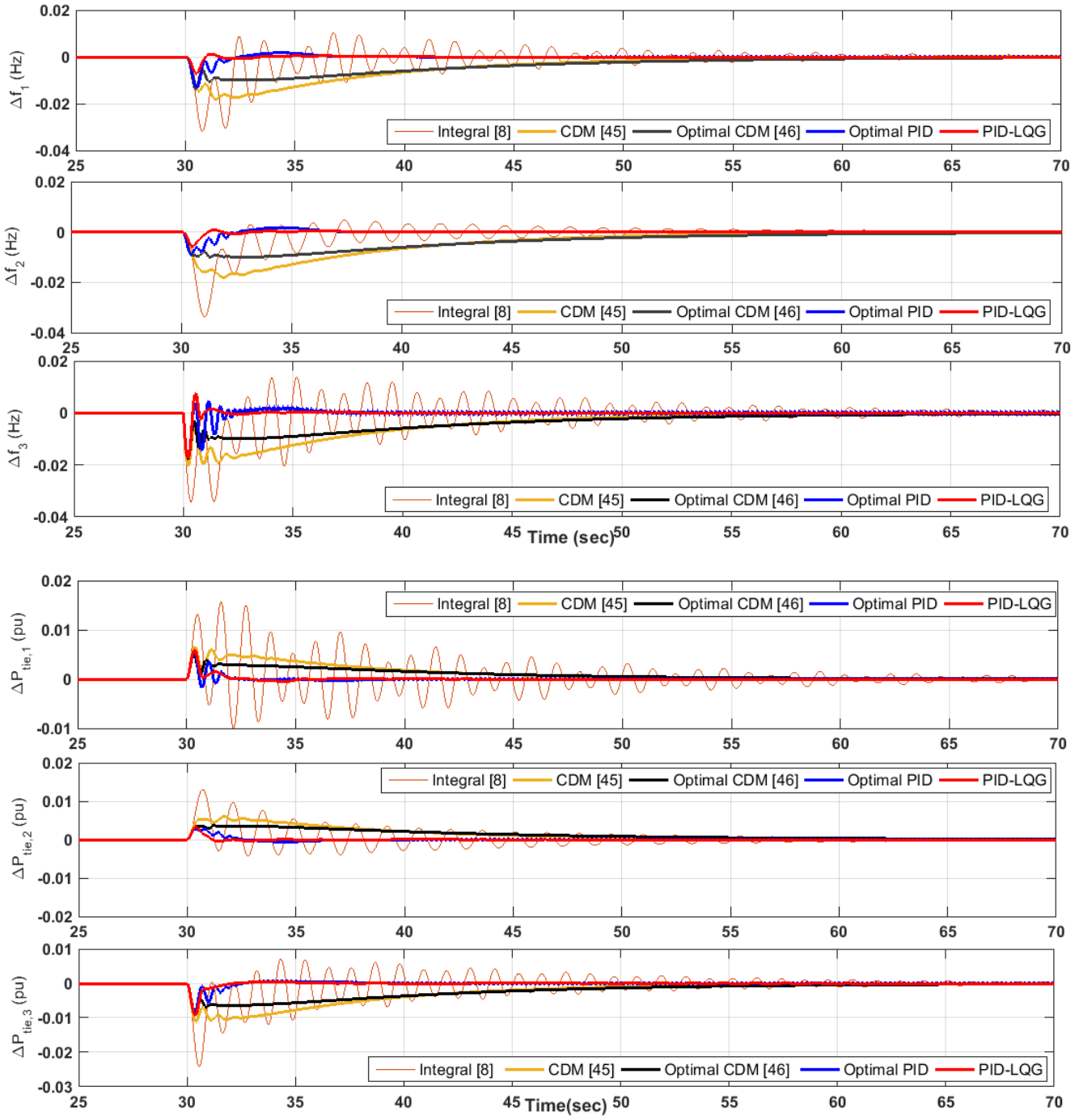

FIGURE 7. The frequency and tie-line power deviations of the studied power system for scenario 1, case A.

TABLE 7. Parameters of the PID and PID-LQG controllers based on the LAPO algorithm at normal system operation.

Parameters	Area (1)		Area (2)		Area (3)	
	Optimal PID	PID-LQG	Optimal PID	PID-LQG	Optimal PID	PID-LQG
k_p	0.0043	-4.2	-9.41	-18	-9.51	-16
k_i	-2.017	-2	-1.86	-4.3	-4.065	-8.2
k_d	-0.577	-2.1	-3.69	-18	-9.764	-13
k_l	-	0.335	-	0.46	-	1.14
k_q	-	0.356	-	0.39	-	0.295
k_r	-	-0.101	-	-0.4	-	-0.13
k_{rg}	-	-0.39	-	0.005	-	-0.3

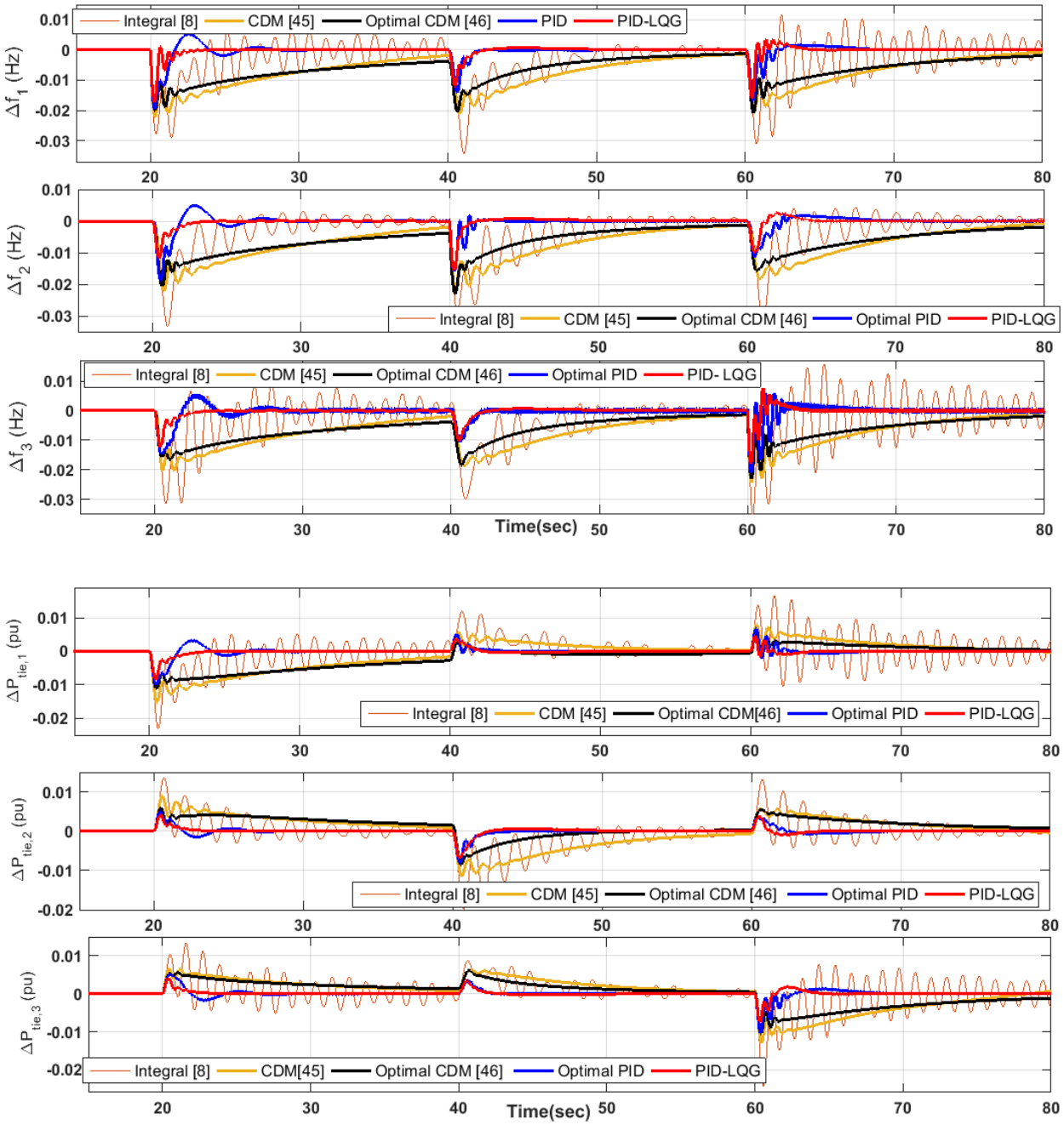

FIGURE 8. The frequency and tie-line power deviations of the studied power system for scenario 1, case B.

TABLE 8. The system operating conditions for scenario 2, case A.

Source	Area	Start time (sec)	Stop time (sec)	Value (pu)
Wind farm 1	Area 1	30	1200	0.038
Wind farm 2	Area 2	90	1200	0.038
Wind farm 3	Area 3	10	1200	0.023
Load disturbance 1	Area 1	60	1200	0.02
Load disturbance 2	Area 2	120	1200	0.02
Load disturbance 3	Area 3	160	1200	0.02

TABLE 9. The system operating conditions for scenario 2, case B.

Source	Area	Start time (sec)	Stop time (sec)	Value (pu)
Wind farm 1	Area 1	initial	1200	0.038
Wind farm 2	Area 2	initial	1200	0.038
Wind farm 3	Area 3	initial	1200	0.023
Load disturbance 1	Area 1	60	1200	0.02
Load disturbance 2	Area 2	120	1200	0.02
Load disturbance 3	Area 3	160	1200	0.02

TABLE 10. The optimal values of the studied controllers with system parameters variation.

Parameters	Area (1)		Area (2)		Area (3)	
	Optimal PID	PID-LQG	Optimal PID	PID-LQG	Optimal PID	PID-LQG
k_p	- 0.457	- 0.4	- 2.411	- 19	- 0.717	-19
k_i	- 0.897	- 1.1	- 8.419	- 5	- 1.563	-9
k_d	- 0.344	- 0.6	- 3.05	- 16	- 1.14	-7.3
k_l	-	1.99	-	2	-	1.99
k_q	-	0.014	-	1.915	-	1.98
k_r	-	- 0.49	-	-0.59	-	1.73
k_{rg}	-	- 0.55	-	-0.51	-	- 0.59

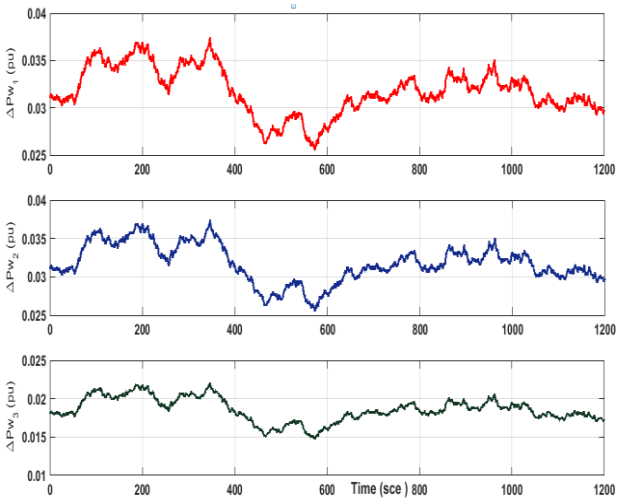

FIGURE 9. The wind power fluctuations of three wind farms.

equation [44].

$$K = -R^{-1}\acute{B}P \tag{25}$$

Referring to the expression of the system input and the second order system taking in consideration the intervals of inputs and finding the state feedback gain according to this relation:

$$\frac{Y(s)}{U(s)} = \frac{a}{s^2 + b_1 s + b_2} = \frac{E(s)}{U(s)} \tag{26}$$

Then, finding the state space model as follows:

$$\begin{bmatrix} \dot{x}_1 \\ \dot{x}_2 \\ \dot{x}_3 \end{bmatrix} = \begin{bmatrix} 0 & 1 & 0 \\ 0 & 0 & 1 \\ 0 & -b_1 & -b_2 \end{bmatrix} \begin{bmatrix} x_1 \\ x_2 \\ x_3 \end{bmatrix} + \begin{bmatrix} 0 \\ 0 \\ a \end{bmatrix} U \tag{27}$$

From (27), the matrices A and B can expressed as follows:

$$A = [[space]] \begin{bmatrix} 0 & 1 & 0 \\ 0 & 0 & 1 \\ 0 & -b_1 & -b_2 \end{bmatrix}, \quad B = \begin{bmatrix} 0 \\ 0 \\ a \end{bmatrix} \tag{28}$$

By resolving (25), using the values of matrix B.

$$k = -R^{-1}B^T P = -R^{-1} \begin{bmatrix} 0 & 0 & a \end{bmatrix} \begin{bmatrix} P_{11} & P_{12} & P_{13} \\ P_{21} & P_{22} & P_{23} \\ P_{31} & P_{32} & P_{33} \end{bmatrix}$$
$$= -R^{-1}a \begin{bmatrix} P_{13} & P_{23} & P_{33} \end{bmatrix} = -\begin{bmatrix} k_l & k_q & k_r \end{bmatrix} \tag{29}$$

After selecting the value of feed gain matrix, we should select the value of Kalman gain matrix (L) that responsible to minimize the covariance estimation error $R_e(t,t)$.

$$R_e(t,t) = E[e_0(t).e_o^T(t)] \tag{30}$$

Here, the $e_0(t)$ estimated error can express as follows:

$$e_0(t) = x(t) - x_0(t). \tag{31}$$

According to input of the system, the state equation of Kalman filter can be expressed as follows:

$$x_0(t) = Ax_o(t) + Bu(t) + L[Y(t) - cx_0(t) - Du(t)] \tag{32}$$

By compensating (31), in (32), and finding the optimal estimation error as follows:

$$\dot{e}_0(t) = [A - LC]\, e_0(t) + Fv(t) - Lz(t) \tag{33}$$
$$w(t) = Fv(t) - Lz(t) \tag{34}$$

Then, summarizing (33), and (34), as follows:

$$\dot{e}_0(t) = Ae_0(t) + w(t) - LCe_0(t) \tag{35}$$

According to the Riccatic equation and then the covariance of estimation error can be express as:

$$\frac{dR_e^0(t,t)}{d(t)} = A \cdot R_e^0(t,t) + R_e^0(t,t) \cdot A^T - R_e^0(t,t) \cdot C^T \cdot Z^{-1}(t) R_e^0(t,t) + FV(t)F^T \tag{36}$$

From the matrix Riccatic equation, the value of is $R_e^0(t,t)$ found out and then the value of (L) is found out by the below equation:

$$L = R_e^0.C^T.Z^{-1}. \tag{37}$$

Now, combining the two resulted gains K and L to form the optimal LQG controller. Then, the optimal state-space realization of LQG controller can be expressed as follows:

$$\acute{X}_0 = [A - BX - LC + LDK]\, X_0 + LY. \tag{38}$$

According to figure 4, the proposed controller depends on the weighting matrixes Q and R which are responsible to obtain the gains for the LQG controller and the PID controller gains.

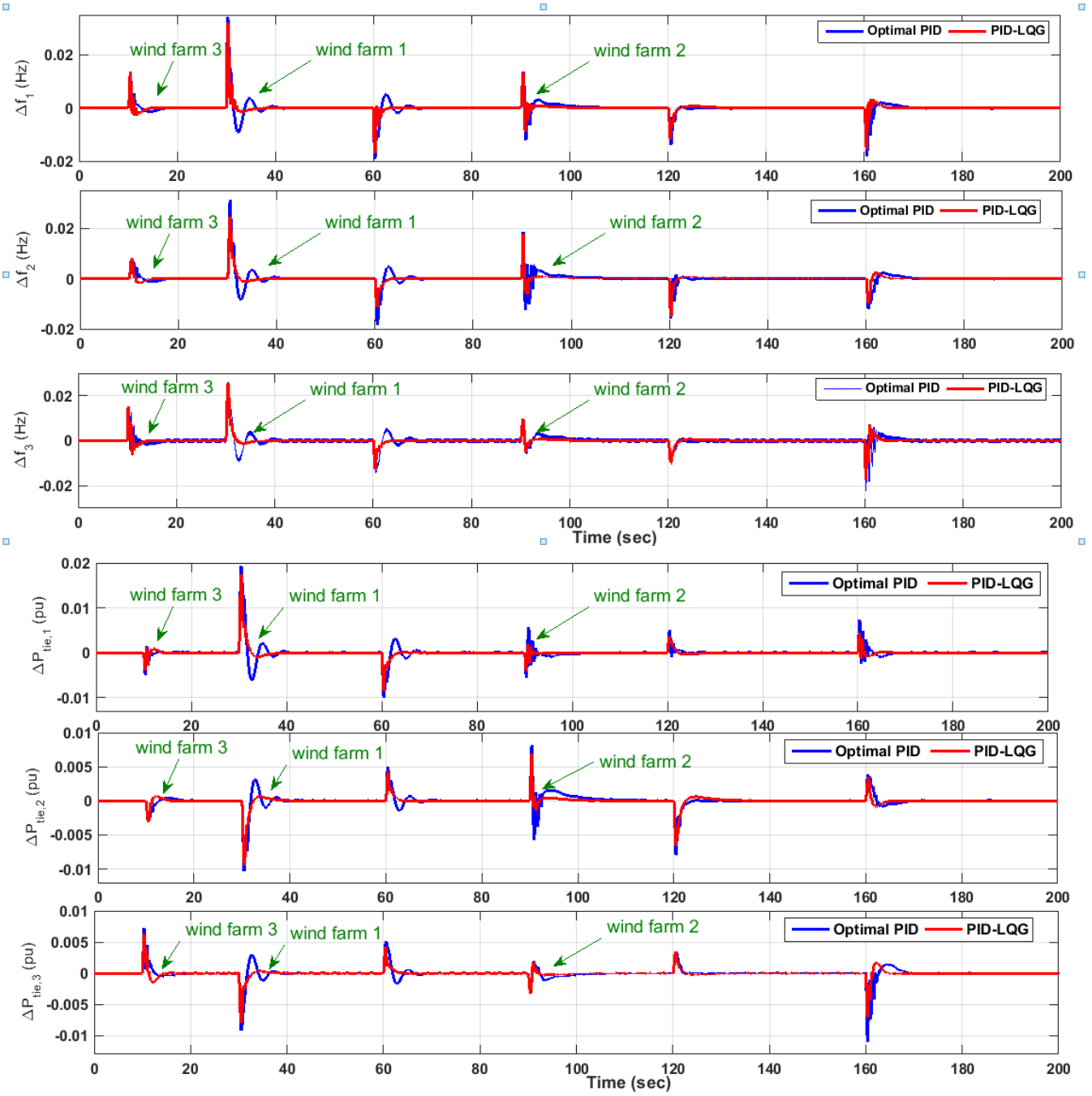

FIGURE 10. The frequency and tie-line power deviations of the studied power system for scenario 2, case A.

B. LIGHTNING ATTACHMENT PROCEDURE OPTIMIZER

LAPO is an algorithm that simulates the lightning formation in natural where cloud contains a huge amount of charges, this leads to the formation of downward leaders and therefore the upward leaders that combined at stick point [31]. The steps of the LAPO algorithm expressed in code as shown in Table 5. The procedure of formulating the LAPO technique is scheduled according to the following procedures:

Step1: Initializing the population

The electric field of a checkpoint which is the solution's fitness is determined according to the objective function

$$F_{ts}^{i} = obj(X_{ts}^{i}) \tag{39}$$

Here, X_{ts}^{i} is the initial check point and is determined according to (40) and considered as downward leader:

$$X_{ts}^{i} = X_{min}^{i} + \left(X_{max}^{i} - X_{min}^{i}\right) \times rand \tag{40}$$

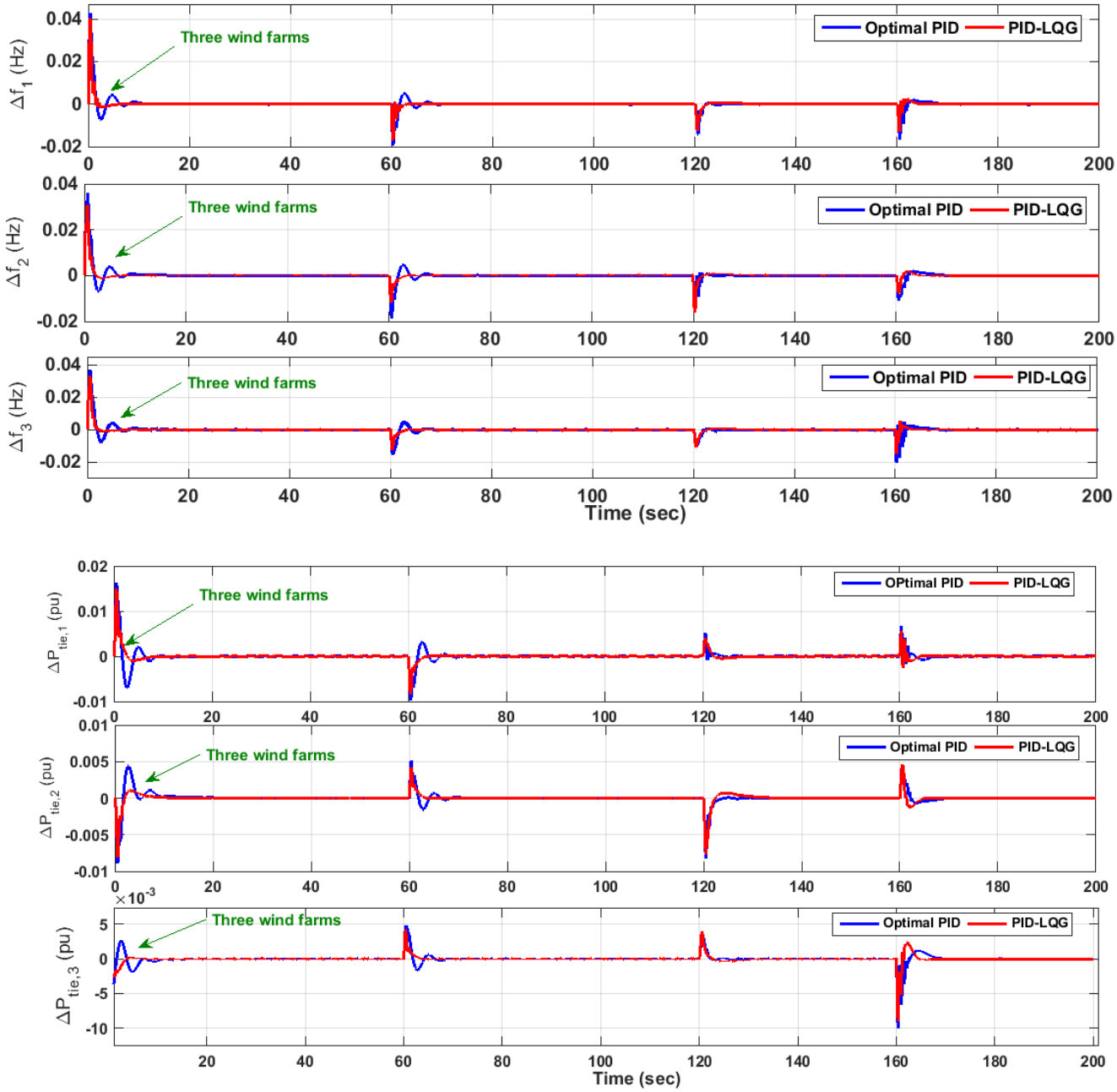

FIGURE 11. The frequency and tie-line power deviations of the studied power system for scenario 2, case B.

The initial check point is depended on the lower bound, the upper bound and randomly variable. Moreover, the value of rand is considered between [0-1]. The objective function of the primary spots can be premeditated as follows:

Step 2: Determine the afterward jump

In this step, the averages of all initial check points is obtained as follow:

$$X_{avr} = mean(X_{ts}) \tag{41}$$

Then, the objective function of these are determined accordingly the following:

$$F_{avr} = obj(X_{avr}) \tag{42}$$

The forward jump is chosen according to the comparison of the value of check point i and the random point j.

First situation, where $F_j < F_{avr}$ the forward jump can determine according to equation (43):

$$X^i_{ts_{new}} = X^i_{ts} + rand \times \left(X_{avr} + A^j_{PS}\right) \tag{43}$$

Second situation, where $F_j > F_{avr}$ the forward jump can determine according to (44):

$$X^i_{ts\_new} = X^i_{ts} - rand \times \left(X_{avr} + X^j_{PS}\right) \tag{44}$$

Step 3: Performing new check point

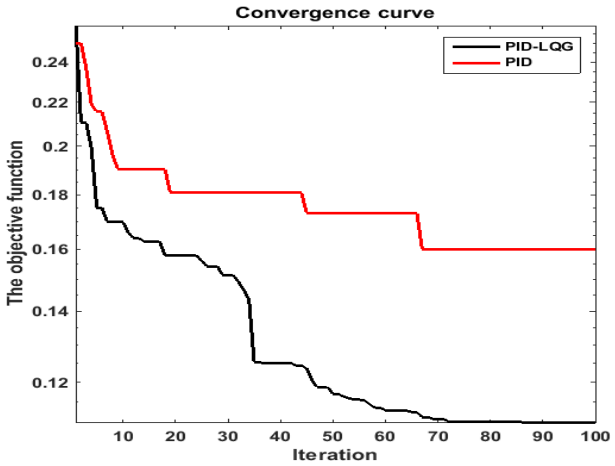

FIGURE 12. Convergence curve for system parameters variations.

All the afterward check points checked according the value of its electric field as follow

IF $F^i_{ts\_new} < F^i_{ts}$ the check point selected as follow:

$$X^i_{ts} = X^i_{ts\_new} \tag{45}$$

Otherwise $F^i_{ts\_new} < F^i_{ts}$ the check point selected as follow:

$$X^i_{ts\_new} = X^i_{ts} \tag{46}$$

Step 4: Leader Upward Movement

Different from the previous consideration for all the previous steps, the check points are considered upward leader and their move depend on charging downward leader. Then, an exponent factor (S) is determined according to the following equation:

$$S = 1 - (\frac{t}{t_{max}}) \times exp(-\frac{t}{t_{max}}) \tag{47}$$

The pervious operator depends on iteration number t and maximum iterations t_{max}. Thus, the next step of check point where is considered as upward leader is formulated as shown in equation (48):

$$X^i_{ts\_new} = X^i_{ts\_new} + rand \times S \times \left(X^i_{best} - X^i_{worst}\right) \tag{48}$$

X^i_{best} is the best solution, while X^i_{worst} is the worst solution.

Step 5: finding the optimal solution

Lightning occurs as soon as up leader combined with down leader and this led to a point which known as striking point. This referring to the optimal solution.

C. PROPOSED CONTROLLER BASED ON THE LAPO ALGORITHM

In this study, the proposed PID-LQG controller is applied to enhance frequency stability in a three-area power system. The proposed controller parameters have been designed optimally by using the LAPO algorithm. The LAPO algorithm serves as a tool to tune the weighting matrices values Q_i and R_i, which are reasonable to select these parameters (k_{li}–k_{qi} – k_{ri} - k_{gi}), and the (k_{pi}– k_{ii}- k_{di}) in each area. Moreover, the flow chart of the LAPO algorithm procedures in selecting the parameters of the proposed controller is shown in figure 5.

The integral time-square error (ITSE) is chosen as single objective function. Moreover, the optimal setting of the LAPO algorithm is listed in Table 6. The optimization process is repeated more than 20 times to yield a minimum fitness value to minimize the deviations of frequency and tie-line power. The model of the ITSE objective function is described as follows:

$$ITES = \int_0^{tsim} (\Delta f_1)^2 + (\Delta f_2)^2 + (\Delta f_3)^2 + (\Delta P_{tie,1})^2 + (\Delta P_{tie,2})^2 + (\Delta P_{tie,3})^2 .dt \tag{49}$$

Here, t_{sim} is the simulation time and Δf_i the deviation of frequency for i- area and $\Delta P_{tie,i}$ the tie-line power for i- area for the studied power system.

Therefore, the proposed controller (PID- LQG) gains constraints are described in (50).

$$\begin{cases} K_p^{min} \le K_p \le K_p^{\max} \\ K_d^{min} \le K_d \le K_d^{\max} \\ K_i^{min} \le K_i \le K_i^{\max} \\ Q^{min} \le Q \le Q^{\max} \\ R^{min} \le R \le R^{\max} \end{cases} \tag{50}$$

IV. SIMULATION STUDY

Computer simulations have been carried out for a three-area interconnected power system considering the high penetration level of wind energy and nonlinearities as shown in Figure 2. Moreover, the GDB is adjusted at 0.05% and GRC to be 10% per minute. The robustness and effectiveness of the proposed controller is validated by comparing its performance with; integral controller [8], CDM controller [45], optimal CDM controller [46], and optimal PID controller based on the LAPO algorithm. The simulation process and results have been carried out using MATLAB/Simulink ®software. Moreover, the LAPO code is written by M-file and interface with the system model to implement the optimization process. In this study, the load profile is assumed to be step change disturbance which can be represented by losses of generation unit or sudden massive loading switch off. Graphical and numerical simulation results are discussed for three scenarios as follows:

Scenario 1. Performance analysis of the studied power system without wind power penetration.

In this scenario, the performance of the studied power system is tested at nominal system parameters without wind power penetration. The optimal values based on the LAPO algorithm for the proposed PID-LQG controller and the optimal PID controller are listed in Table 7. Figure 6 shows the convergence profile of the optimal PID controller and the proposed PID-LQG controller. The simulation results of this scenario are performed for two different cases as follows:

Case A: a 2 % step load change is applied in area-3 at 30 sec. The frequency and tie line power deviations of

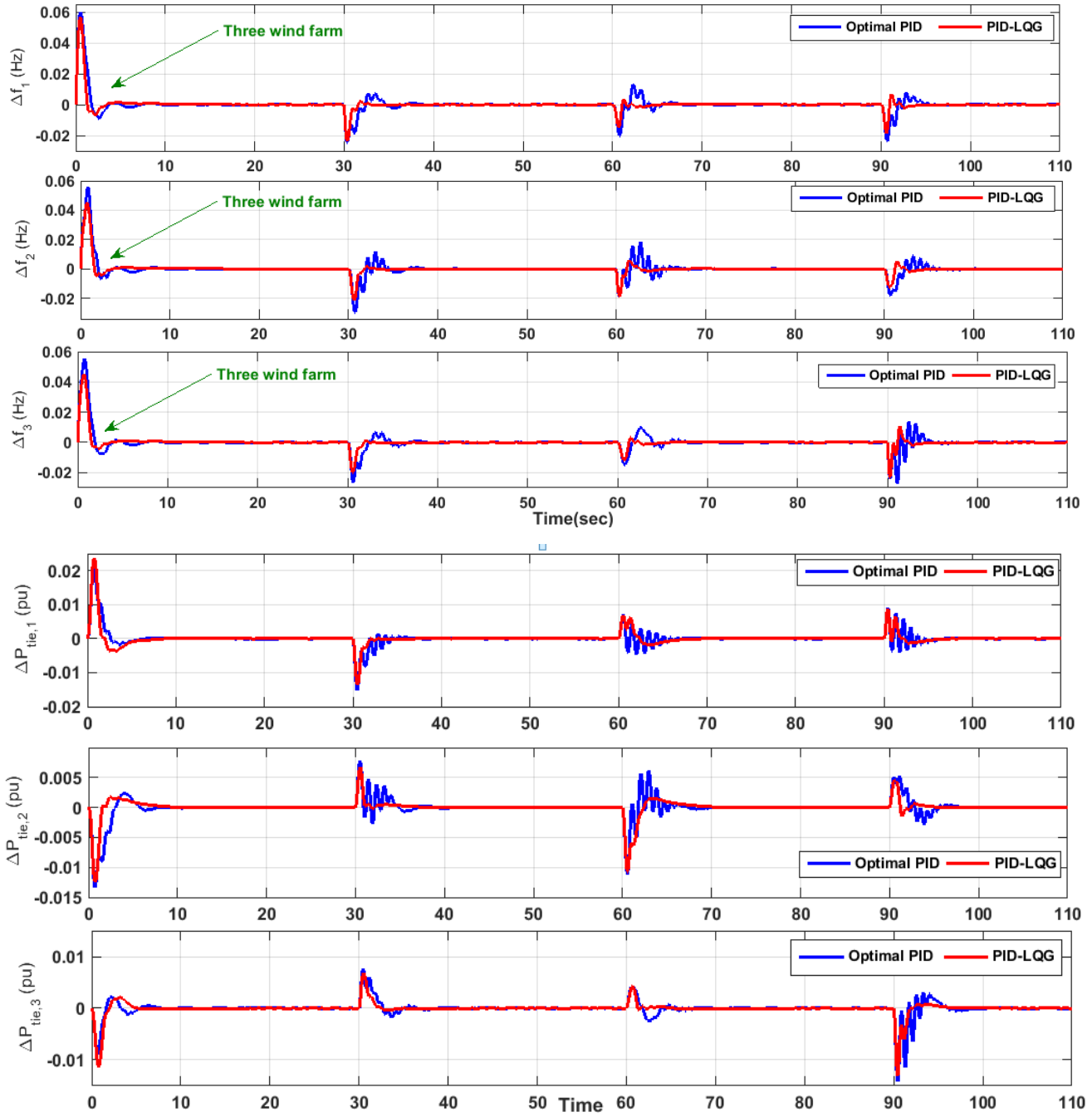

FIGURE 13. The frequency and tie-line power deviations of the studied power system for scenario 3.

the studied power system for case1 with different control schemes are shown in Figure 7. According to the simulation result of this scenario, the proposed controller gives better performance in comparison with other control strategies (i.e., optimal CDM controller, CDM controller, optimal PID-based LAPO algorithm, and integral controller) in terms of settling time, overshoot and under shoot.

Case B: a 2 % step load change is applied in area-1 at 20 sec, area-2 at 40 sec, and area-3 at 60 sec, respectively. The frequency and tie-line power deviations of the studied power system for this case study with different control schemes are presented in Figure 8. The proposed control strategy has a small value of oscillation compared with other control strategies.

Scenario 2. Performance analysis of the studied power system considering high wind power penetration.

In this scenario, the performance of the studied power system is tested at nominal system parameters considering high wind power penetration. The power fluctuations of the three wind farms are shown in Figure 9. The simulation results are discussed in for different two cases as follows:

Case A: the operating conditions of wind farms and load disturbances for this case are listed in Table 8. Figure 10 shows the frequency and tie-line power deviations of the studied three-area interconnected power system considering wind energy with different control schemes (i.e. the proposed PID-LQG controller-based the LAPO algorithm, and optimal PID controller-based the LAPO algorithm) for this case. The proposed PID-LQG controller-based LAPO algorithm has better performance than the PID controller-based the LAPO algorithm as its ability in minimizing deviation result from wind farms penetrations and load disturbance in each area.

Case B: the effect of wind power penetration occurs from the initial simulation time. The operating conditions of wind farms and load disturbances for this case are listed in Table 9. The frequency and tie-line power deviations of the studied three-area interconnected power system considering wind energy with different control schemes are shown in Figure 11. It is clear that the proposed PID-LQG controller-based LAPO algorithm eliminates deviations in frequency and tie-line power compared to the optimal PID-based LAPO algorithm in the face of wind farms penetration at the same time.

Scenario 3. Performance analysis of the studied power system considering high wind power penetration and system uncertainties

The performance of the studied three-area interconnected power system is tested with the proposed PID-LQG controller under the severe case. The system parameters changed as follows, the governor and turbine time constants of each area are increased from their values to $T_{g1} = 0.105$ sec, $T_{t1} = 0.785$ sec, $T_{g2} = 0.105$ sec, $T_{t2} = 0.6$ sec, $T_{g3} = 0.15$ sec and $T_{t3} = 0.7$ sec. The optimal values of the PID-LQG controller and the conventional PID controller based on the LAPO algorithm are listed in Table 10. The convergence curve for this test is shown in figure 12.

The robustness of the proposed PID-LQG controller-based LAPO algorithm is examined under the worst-case which maybe occur to the system. The operating conditions of wind farms and load disturbance are considered as listed in Table 9. Figure13 shows the frequency and tie-line power deviations of the studied three-area interconnected power system for this scenario. The proposed PID-LQG controller based on the LAPO algorithm accomplishes frequency deviations better than the optimal PID controller-based LAPO algorithm in less settling time. The performance of the proposed controller has the best values in terms of maximum overshoot and undershoot.

V. CONCLUSION

This study has proposed a robust control strategy based on a combination of the PID controller and the LQG approach, referred to as the PID-LQG controller, for frequency stability enhancement in a three-area interconnected power system considering high wind power penetration. The parameters of the proposed controller were determined based on the LAPO algorithm due to it has many merits such as good exploration, exploitation abilities, and doesn't require any specific parameters. However, the proposed algorithm has drawback of slow convergence speed. On the other hand, the LQR approach has proven highly worthy in many engineering applications due to it provides fast convergence and less mathematical intricacy. Where it was recently applied with a view to achieving the best performance of a wind energy conversion system through adjusting the machine-and the grid-side converter/inverter. The simulation results indicated that the proposed PID-LQG controller gives better performance than other control techniques (i.e. conventional controller – CDM controller- Optimal CDM controller- Optimal PID controller based LAPO algorithm) against loads/RESs perturbations and system uncertainties.

ACKNOWLEDGMENT

The authors would like to acknowledge the support of the Chilean Council of Scientic and Technological Research, ANID/Fondap/15110019.

REFERENCES

[1] M. S. Hossain, N. A. Madlool, N. A. Rahim, J. Selvara, A. K. Pandey, and A. F. Khan, "Role of smart grid in renewable energy: An overview," *Renew. Sustain. Energy Rev.*, vol. 60, pp. 1168–1184, Jul. 2016.
[2] R. Babu and A. Pachiyappan, "Wind energy conversion system—A technical review," *J. Eng. Sci. Technol.*, vol. 8, no. 4, pp. 493–507, 2013.
[3] C. Tian, A. Maleki, S. Motie, A. Yavarinasab, and M. Afrand, "Generation expansion planning by considering wind resource in a competitive environment," *J. Thermal Anal. Calorimetry*, vol. 139, pp. 2847–2857, Dec. 2019.
[4] S. Motie, F. Keynia, M. R. Ranjbar, and A. Maleki, "Generation expansion planning by considering energy-efficiency programs in a competitive environment," *Int. J. Electr. Power Energy Syst.*, vol. 80, pp. 109–118, Sep. 2016.
[5] G. Magdy, G. Shabib, A. A. Elbaset, and Y. Mitani, "Renewable power systems dynamic security using a new coordination of frequency control strategy based on virtual synchronous generator and digital frequency protection," *Int. J. Electr. Power Energy Syst.*, vol. 109, pp. 351–368, Jul. 2019.
[6] A. Maleki, M. G. Khajeh, and M. Ameri, "Optimal sizing of a grid independent hybrid renewable energy system incorporating resource uncertainty, and load uncertainty," *Int. J. Electr. Power Energy Syst.*, vol. 83, pp. 514–524, Dec. 2016.
[7] W. Zhang, A. Maleki, and M. A. Rosen, "A heuristic-based approach for optimizing a small independent solar and wind hybrid power scheme incorporating load forecasting," *J. Cleaner Prod.*, vol. 241, Dec. 2019, Art. no. 117920.
[8] H. Bevrani, *Robust Power System Control*. New York, NY, USA: Springer, 2014.
[9] R. Shankar, S. R. Pradhan, K. Chatterjee, and R. Mandal, "A comprehensive state of the artliterature survey on LFC mechanism for power systems," *Renew. Sustain. Energy Rev.*, vol. 76, no. 1, pp. 185–207, 2017.
[10] H. A. Yousef, K. Al-Kharusi, M. H. Albadi, and N. Hosseinzadeh, "Load frequency control of a multi-area power system: An adaptive fuzzy logic approach," *IEEE Trans. Power Syst.*, vol. 29, no. 4, pp. 1822–1830, Jul. 2014.
[11] J. Liu, Q. Yao, and Y. Hu, "Model predictive control for load frequency of hybrid power system with wind power and thermal power," *Energy*, vol. 172, pp. 555–565, Apr. 2019.
[12] D. Xu, J. Liu, X.-G. Yan, and W. Yan, "A novel adaptive neural network constrained control for a multi-area interconnected power system with hybrid energy storage," *IEEE Trans. Ind. Electron.*, vol. 65, no. 8, pp. 6625–6634, Aug. 2018.
[13] V. Kushwaha, K. Pandey, S. Sehrawat, and D. Sharma, "Adaptive neuro-fuzzy based load frequency controller for three area inter-connected hydro-thermal power system," in *Proc. 2nd Int. Innov. Appl. Comput. Intell. Power, Energy Controls Their Impact Humanity (CIPECH)*, Ghaziabad, India, Nov. 2016, pp. 34–38.
[14] H. Li, X. Wang, and J. Xiao, "Adaptive event-triggered load frequency control for interconnected microgrids by observer-based sliding mode control," *IEEE Access*, vol. 7, pp. 68271–68280, 2019.

[15] K. Lu, W. Zhou, G. Zeng, and Y. Zheng, "Constrained population extremal optimization-based robust load frequency control of multi-area interconnected power system," *Int. J. Electr. Power Energy Syst.*, vol. 105, pp. 249–271, Feb. 2019.
[16] A. Abazari, H. Monsef, and B. Wu, "Coordination strategies of distributed energy resources including FESS, DEG, FC and WTG in load frequency control (LFC) scheme of hybrid isolated micro-grid," *Int. J. Electr. Power Energy Syst.*, vol. 109, pp. 535–547, Jul. 2019.
[17] H. M. Hasanien and A. A. El-Fergany, "Salp swarm algorithm-based optimal load frequency control of hybrid renewable power systems with communication delay and excitation cross-coupling effect," *Electr. Power Syst. Res.*, vol. 176, Nov. 2019, Art. no. 105938.
[18] K. S. Rajesh and S. S. Dash, "Load frequency control of autonomous power system using adaptive fuzzy based PID controller optimized on improved sine cosine algorithm," *J. Ambient Intell. Humanized Comput.*, vol. 10, no. 6, pp. 2361–2373, Jun. 2019.
[19] E. S. Ali and S. M. Abd-Elazim, "Bacteria foraging optimization algorithm based load frequency controller for interconnected power system," *Int. J. Electr. Power Energy Syst.*, vol. 33, no. 3, pp. 633–638, Mar. 2011.
[20] E. Ali and A. Abd-Elaziz, "Cuckoo search algorithm based load frequency controller design for nonlinear interconnected power system," *Int. J. Electr. Power Energy Syst.*, vol. 73, pp. 623–643, Dec. 2015.
[21] M. Elsisi, M. Soliman, M. A. S. Aboelela, and W. Mansour, "Bat inspired algorithm based optimal design of model predictive load frequency control," *Int. J. Electr. Power Energy Syst.*, vol. 83, pp. 426–433, Dec. 2016.
[22] B. V. S. Acharyulu, M. Banaja and P. K. Hota, "Comparative performance analysis of PID controller with filter for automatic generation control with moth-flame optimization algorithm," in *Applications of Artificial Intelligence Techniques in Engineering* (Advances in Intelligent Systems and Computing), vol. 698, H. Malik, S. Srivastava, Y. Sood, and A. Ahmad, Eds. Singapore: Springer, 2019. [Online]. Available: https://doi.org/10.1007/978-981-13-1819-1_48
[23] D. Guha, P. K. Roy, and S. Banerjee, "Binary bat algorithm applied to solve MISO-type PID-SSSC-based load frequency control problem," *Iranian J. Sci. Technol., Trans. Electr. Eng.*, vol. 43, no. 2, pp. 323–342, Jun. 2019.
[24] A. Annamraju and S. Nandiraju, "Coordinated control of conventional power sources and PHEVs using Jaya algorithm optimized PID controller for frequency control of a renewable penetrated power system," *Protection Control Mod. Power Syst.*, vol. 4, no. 1, pp. 4–28, Dec. 2019.
[25] S. S. Dhillon, A. Surabhi, G. Wang, and J. S. Lather, "Automatic generation control of interconnected power systems using elephant herding optimization," in *Intelligent Computing Techniques for Smart Energy Systems* (Lecture Notes in Electrical Engineering), vol. 607, A. Kalam, K. Niazi, A. Soni, S. Siddiqui, A. Mundra, Eds. Singapore: Springer, 2019. [Online]. Available: https://doi.org/10.1007/978-981-15-0214-9_2
[26] H. Ali, G. Magdy, B. Li, G. Shabib, A. A. Elbaset, D. Xu, and Y. Mitani, "A new frequency control strategy in an islanded microgrid using virtual inertia control-based coefficient diagram method," *IEEE Access*, vol. 7, pp. 16979–16990, 2019.
[27] T. Kerdphol, F. S. Rahman, Y. Mitani, M. Watanabe, and S. Kufeoglu, "Robust virtual inertia control of an islanded microgrid considering high penetration of renewable energy," *IEEE Access*, vol. 6, pp. 625–636, 2018.
[28] Y. Han, P. M. Young, A. Jain, and D. Zimmerle, "Robust control for microgrid frequency deviation reduction with attached storage system," *IEEE Trans. Smart Grid*, vol. 2, no. 6, pp. 565–575, Nov. 2015.
[29] H. Bevrani, M. R. Feizi, and S. Ataee, "Robust frequency control in an islanded microgrid: H∞ and μ-synthesis approaches," *IEEE Trans. Smart Grid*, vol. 7, no. 2, pp. 706–717, Mar. 2016.
[30] H. S. Seyed and D. Farsi, "Analysis of load frequency control in a restructured multi-area power system with the Kalman filter and the LQR controller," *AEU-Int. J. Electron. Commun.*, vol. 86, pp. 25–46, Mar. 2018.
[31] G. Shabib, T. H. Mohamed, E. H. Abrdelhameed, and M. Khamies, "An advanced linear quadratic regulator for load frequency control for single area power system," in *Proc. 17th Int. Middle East Power Syst. Conf.*, Mansoura, Egypt, 2015, pp. 1–5.
[32] T. H. Mohamed, G. Shabib, E. H. Abdelhameed, M. Khamies, and Y. Qudaih, "Load frequency control in single area system using model predictive control and linear quadratic Gaussian techniques," *Int. J. Electr. Energy*, vol. 3, no. 3, pp. 141–144, 2015.
[33] S. K. Das, M. Rahman, S. K. Paul, M. Armin, P. N. Roy, and N. Paul, "High-performance robust controller design of plug-in hybrid electric vehicle for frequency regulation of smart grid using linear matrix inequality approach," *IEEE Access*, vol. 7, pp. 116911–116924, 2019.
[34] H. Md Alamgir, "Linear quadratic Gaussian regulator based frequency control of power system to enhance the continuity of power flow," *Amer. J. Eng. Res.*, vol. 8, no. 14, pp. 348–354, 2019.
[35] R. Mizanur, S. Neepa, S. Subrata, and D. Sajal, "PHEV participating in load frequency regulation of interconnected smart grid using integral linear quadratic Gaussian control approach," in *Proc. Int. Conf. Energy Power Eng. (ICEPE)*, Dhaka, Bangladesh, 2019, pp. 1–6.
[36] A. F. Nematollahi, A. Rahiminejad, and B. Vahidi, "A novel physical based meta-heuristic optimization method known as lightning attachment procedure optimization," *Appl. Soft Comput.*, vol. 59, pp. 596–621, Oct. 2017.
[37] A. Foroughi Nematollahi, A. Rahiminejad, and B. Vahidi, "A novel multi-objective optimization algorithm based on lightning attachment procedure optimization algorithm," *Appl. Soft Comput.*, vol. 75, pp. 404–427, Feb. 2019.
[38] H. Youssef, S. Kamel, and M. Ebeed, "Optimal power flow considering loading margin stability using lightning attachment optimization technique," in *Proc. 20th Int. Middle East Power Syst. Conf. (MEPCON)*, Dec. 2018, pp. 1053–1058.
[39] H. Pejman, F. N. Amin, and V. Behrooz, "A novel approach for optimal DG allocation in distribution network for minimizing voltage sag," *Adv. Energy Res.*, vol. 6, no. 1, pp. 55–73, 2011.
[40] G. Magdy, E. A. Mohamed, G. Shabib, A. A. Elbaset, and Y. Mitani, "SMES based a new PID controller for frequency stability of a real hybrid power system considering high wind power penetration," *IET Renew. Power Gener.*, vol. 12, no. 11, pp. 1304–1313, Aug. 2018.
[41] L. Xiangjun, H. Dong, L. Xiaokang, and Y. Tao, "Power quality control in wind/fuel cell/battery/ hydrogen electrolyzer hybrid micro-grid power system," in *Applications and Experiences of Quality Control*, O. Ivanov, Ed. IntechOpen, Nov. 2011.
[42] G. Shabib, E. H. AbdElhameed, and G. Magdy, "Robust digital redesign of continuous PID controller for power system using plant-inputmapping," *WSEAS Trans. Power Syst.*, vol. 13, no. 1, pp. 31–39, 2018.
[43] M. Rahman, S. K. Sarkar, S. K. Das, and Y. Miao, "A comparative study of LQR, LQG, and integral LQG controller for frequency control of interconnected smart grid," in *Proc. 3rd Int. Conf. Electr. Inf. Commun. Technol. (EICT)*, Dec. 2017, pp. 1–6.
[44] K. Adman, O. Yuksel, and C. Huseyin, "The modelling of electric power systems on the state space and controlling of optimal LQR load frequency," *J. Electr. Electron. Eng.*, vol. 9, no. 2, pp. 977–982, 2009.
[45] T. H. Mohamed, G. Shabib, and H. Ali, "Distributed load frequency control in an interconnected power system using ecological technique and coefficient diagram method," *Int. J. Electr. Power Energy Syst.*, vol. 82, pp. 496–507, Nov. 2016.
[46] M. Heshmati, R. Noroozian, S. Jalilzadeh, and H. Shayeghi, "Optimal design of CDM controller to frequency control of a realistic power system equipped with storage devices using grasshopper optimization algorithm," *ISA Trans.*, vol. 97, pp. 202–215, Feb. 2020.

MOHAMED KHAMIES received the B.Sc. and M.Sc. degrees (Hons.) in electrical engineering from Aswan University, Egypt, in 2011 and 2014, respectively, where he is currently pursuing the Ph.D. degree in electrical engineering. Since 2013, he has been an Electrical Engineer with the Ministry of Electricity and Renewable Energy, Egypt. His research interests include power system stability, and control, smart/micro-grid control, renewable energies, and energy storage systems.

GABER MAGDY received the B.Sc. and M.Sc. degrees (Hons.) in electrical engineering from Aswan University, Aswan, Egypt, in 2011 and 2014, respectively, and the Ph.D. degree in electrical engineering from Minia University, Egypt (Home University), and the Kyushu Institute of Technology, Japan (Host University), in 2019. Since 2012, he joined the Department of Electrical Engineering, Faculty of Energy Engineering, Aswan University, first as a Demonstrator (Assistant Researcher), and then an Assistant Lecturer, from 2012 to 2014 and 2014 to 2017, respectively, where he is currently an Assistant Professor. From 2017 to 2019, he was a Researcher with the Department of Electrical and Electronic Engineering, Kyushu Institute of Technology, Japan. His research interests include power system stability, dynamics, and control, digital control, smart/micro-grid control, renewable energies, and energy storage systems.

MOHAMED EBEED HUSSEIN received the B.S. degree from Aswan University, in 2005, the M.S. degree in electrical engineering from South Valley University, in 2013, and the jointly-supervised Ph.D. degree from the Department of Electrical Engineering, Aswan Faculty of Engineering, Aswan University, and the University of Jaen, Spain, in 2018. From 2008 to 2009, he was a Lecturer with the Aswan Technical Institute. From 2009 to 2017, he was a Maintenance Engineer with EFACO Company. He is currently an Assistant Professor with the Department of Electrical Engineering, Faculty of Engineering, Sohag University, Egypt.

FAHD A. BANAKHR (Member, IEEE) received the degree in electronic and industrial control engineering from the University of Nottingham, Trent, U.K., the master's degree in electronic instrumentation systems from The University of Manchester, U.K., and the Ph.D. degree in sensors and instrumentation engineering from Loughborough University, U.K. He is currently a Visitor Lecturer in smart and intelligent instrumentation with the University of Nottingham. His research interests include intelligent and smart sensors, intelligent control systems, the Internet of Things, and artificial intelligence. He is a member of ISA, the IEEE Control Systems (Intelligent Control Systems Technical Committee), and the Institute of Measurements and Control, U.K. He was awarded the High Voltage Association Student Excellence Award from IEEE International Power Modulator and High Voltage Conference, in 2012. He was also awarded the Sir Martin Award for Academic and non-academic achievement from Loughborough University, in 2011. He is the Chairman of the IEEE Internet of Things and Harmonization Middle East Sub Group and the Vice Chairman of the IEEE Smart Transducers for the IoT Working Group.

SALAH KAMEL received the International Ph.D. degree in electrical engineering from the University of Jaen, Spain (Main), and Aalborg University, Denmark (Host), in 2014. He is an Associate Professor with the Department of Electrical Engineering, Aswan University. His research interests include power system analysis and optimization, smart grid, and renewable energy systems.